# Remote Sensing of the Optical Properties of Clouds

Robyn Schofield[1,2], John S. Daniel[2], Susan Solomon[2], H. LeRoy Miller[1,2], Robert W. Portmann[2] and David D. Turner[3]
[1] Cooperative Institute for Research in Environmental Sciences, University of Colorado, 216 UCB, Boulder, CO 80309, USA
[2] Chemistry and Climate Processes, NOAA Earth Systems Research Laboratory, 325 Broadway, Boulder CO 80305, USA
[3] University of Wisconsin - Madison, Dayton Street, Madison, WI 53706, USA
Robyn.Schofield@noaa.gov

## Motivation

Large uncertainties exist in our understanding of how clouds are changing with different aerosol loadings. The first aerosol indirect effect is outlined in the schematic given below in Figure 1 [Rosenfeld, 2000]. Twomey [1974] outlined that for a constant liquid water content (LWC), under low aerosol loadings there would be fewer cloud condensation nuclei (CCN), thus larger but fewer droplets. Conversely, high aerosol loads would be associated with more CCN, hence more particles but of smaller radii. Smaller particles are actually have a lower albedo than larger particles, but the higher number of particles causes the associated cloud albedo to have a net increase over an unpolluted case. Thus to assess the indirect effect of aerosol on clouds a measure of the LWC and the effective radius are necessary, as well as concurrent aerosol measurements.

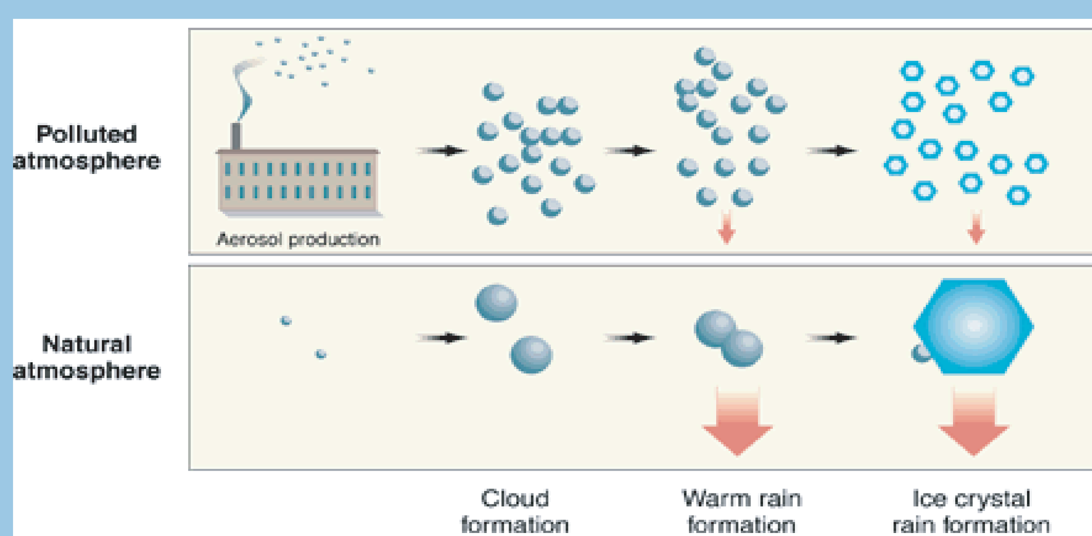


*Figure 1: Schematic of the aerosol indirect effect, taken from [Rosenfeld, 2000].*

Much of our current understanding of cloud microphysical properties is from in situ aircraft measurements from field campaigns. These studies are however of limited temporal and spatial extent. For studies over longer time periods and for global studies remote sensing techniques are necessary. Cloud optical properties can be assessed remotely using LWP (which is the LWC integrated over the vertical path) and effective radius measurements. The path integrated liquid water path (PLWP) is the LWC multiplied by the optical path which is a function of the radiative properties of the atmosphere. The path through the atmosphere is calculated using a radiative transfer algorithm as a function of LWP, solar zenith angle and radius of the scattering liquid particles ($r_{eff}$) such that the following relationship can be written:

$$PLWP = Path(r_{eff}, SZA, LWP) \times LWP$$

LWP retrievals currently use passive microwave radiometer measurements, with an error of 20 $gm^{-2}$ and and bias of 15-30 $gm^{-2}$ [Marchand, et al., 2003; Min and Duan, 2005]. To derive the effective radius current approaches use microwave LWP retrievals in combination with narrowband and broadband diffuse measurements [Kim, et al., 2003; Min and Harrison, 1996], and difference cloud indices [Oreopoulos, et al., 2000]. This work outlines the derivation of effective radius and LWP using a combination of intensity measurements with PLWP measurements and compares these results with those using LWP derived from combining the microwave and PLWP measurements.

Microwave radiometer measurements are conducted as part of the Atmospheric Radiation Measurement (ARM) program (http://www.arm.gov/). The microwave radiometer detects radiation at 23.8 Ghz and 31.4 Ghz. The 23.8 Ghz band is chosen because at this frequency the vapor emission does not change with pressure (a so-called hinge point), thus the water vapor information is primarily provided by this frequency. The 31.4 Ghz band is chosen for the liquid water emission, which is a continuum increasing with frequency, thus liquid water emission dominates the 31.4 Ghz measurement.

The effective radius is retrieved for the combined microwave LWP and NIR PLWP measurements using optimal estimation with a Levenberg-Marquardt combination of steepest descent and inverse Hessian to invert the path enhancement to radius [Rodgers, 2000]. The optimal estimation retrieval scheme takes into account the measurements, their uncertainities, prior knowledge of the effective radius and its uncertainty. The relationship between radius, SZA, LWP and path enhancement (equation 1) is calculated using Mie calculations [Wiscombe, 1980] coupled with DISORT2.0 [Stamnes, et al., 1988], a radiative transfer algorithm. Figure 4 outlines the microwave retrieval of LWP and precipitable water vapor (PWV) and the combined microwave LWP and NIR PLWP retrieval of radius.

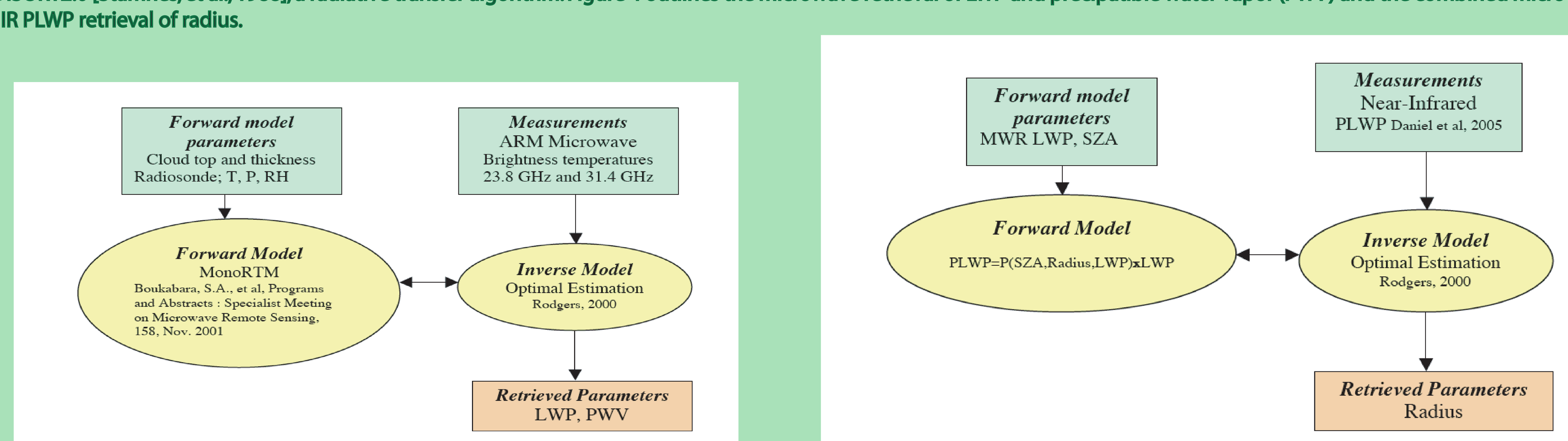


*Figure 4: Left panel displays the algorithm flow chart for microwave retrievals of LWP and PWV. Rightpanel displays the algorithm flow chart for the combined microwave and PLWP retrieval of radius.*

Combining the intensity measurements with the NIR PLWP to retrieve both LWP and radius is also performed using optimal estimation with a Levenberg-Marquardt approach. The intensity like the path (used to obtain PLWP) is a function of SZA, LWP, surface albedo and effective radius. This combination of measurements is chosen due to the different sensivities that the PLWP and intensities have to LWP.

## Results: Case study - Barrow, Alaska, 2004

Both radius retrieval techniques were applied to ground-based observations of clouds made during September at Barrow, Alaska, 2004. Unlike the photo depicting fine weather (Figure 5) Barrow was chosen for its consistent cloud cover during September, where marine boundary layer stratus cloud cover is routinely in liquid water form, turning to ice at colder periods in late September.

*Figure 5. Left - the observation site at Barrow, Alaska looking toward the ocean. Right - the winglet containing the entrance optics for the spectral observations used to obtain the intensity and PLWP measurements.*

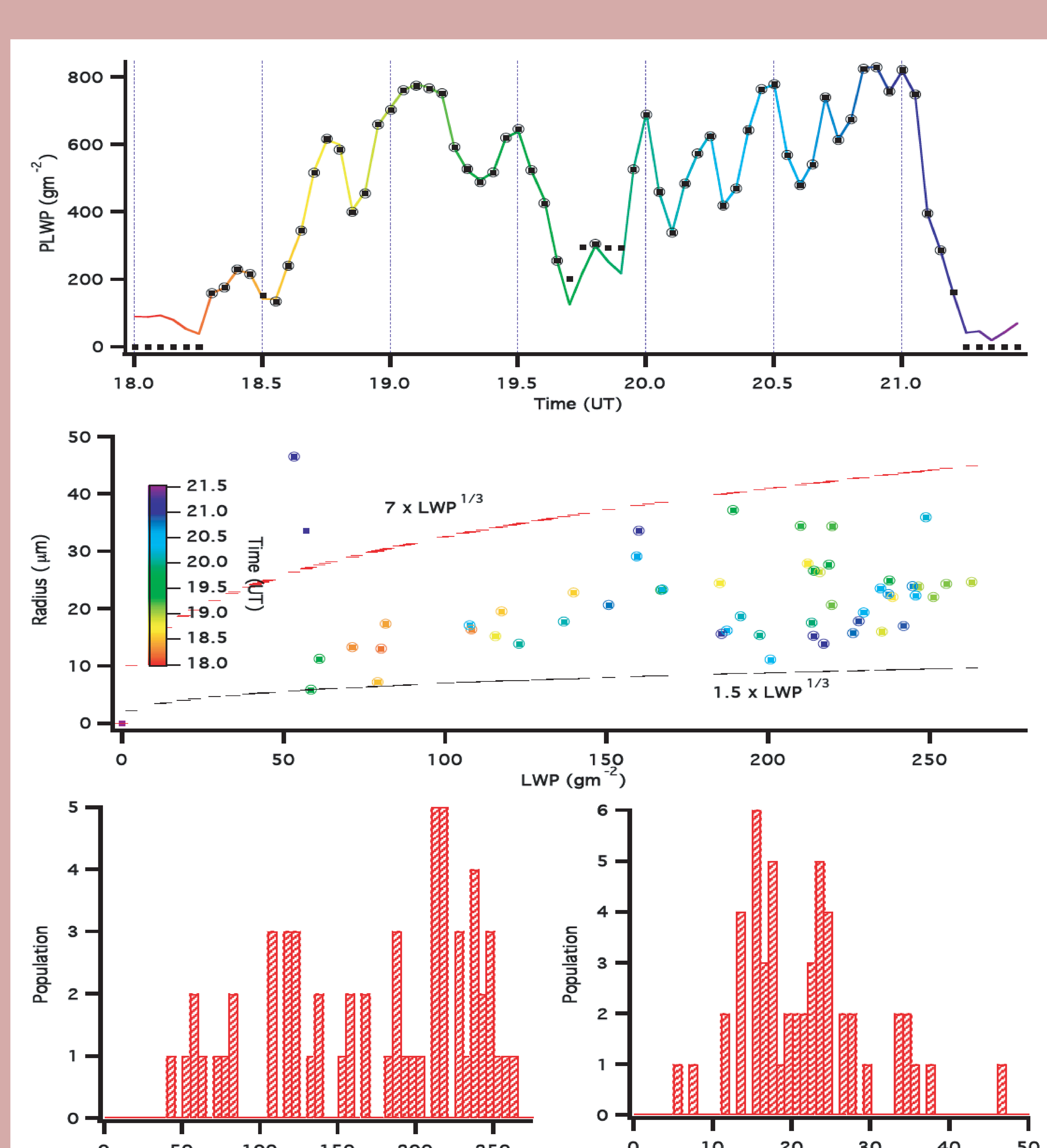


*Figure 6. Combined microwave and PLWP retrieval results. Upper panel depicts the PLWP for 14th September, 2004 from 18-21.5 UT. The middle panel displays the retrieved radii and the lower panels give the distribution of the LWP (microwave product) and radii.*

## Method

Microwave emission, infrared absorption and intensity measurements are used to examine clouds. Combining these different measurements with radiative transfer models, radius and liquid water path information is able to be derived. Remote sensing of clouds at different wavelengths exploits the different radiative properties of the atmosphere for photons of different energies. In the near infrared, measurements are conducted using spectroscopy in the wavelength region between 900 and 1700 nm. Solar radiation is attenuated due to water (liquid and ice) and oxygen absorption, as displayed in figure 2 [Daniel, et al., 2005].

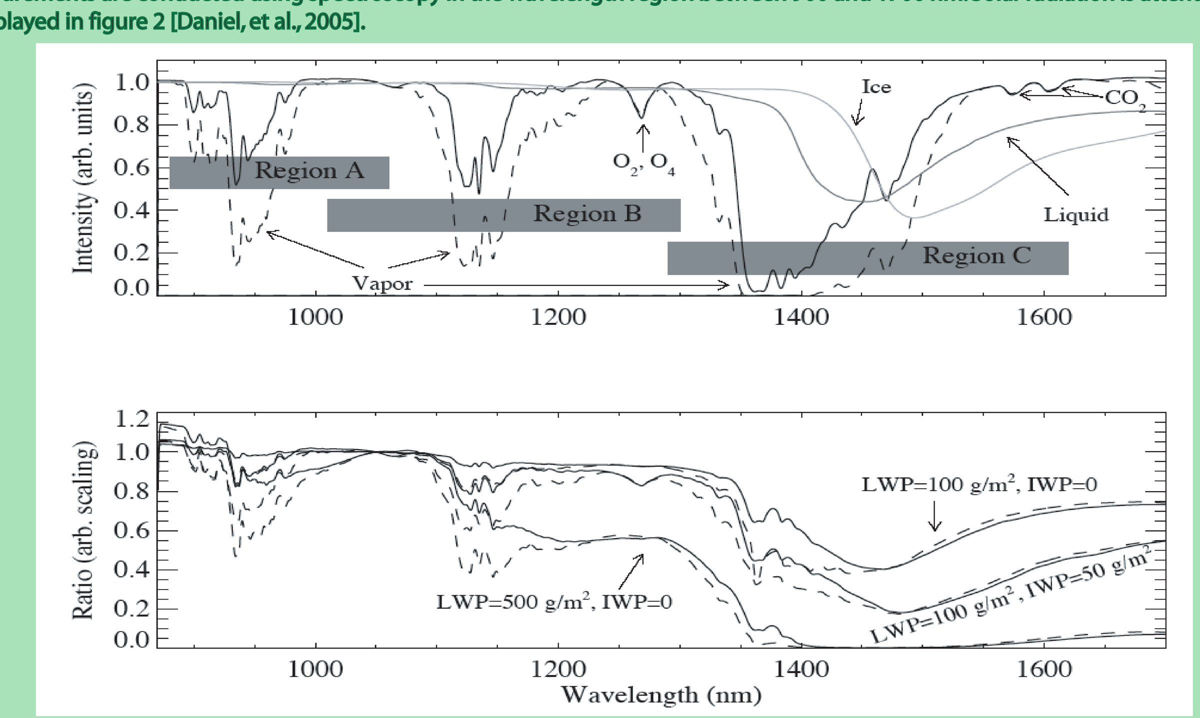


*Figure 2: (Upper panel) Spectral ranges of the three retrieval bands considered. Calculated direct transmission spectra through bulk liquid and ice of 0.25 mm thickness along with clear-sky zenith normalized radiances. (Lower panel) Calculated zenith-sky spectral ratios under pure liquid or liquid and ice clouds assuming a liquid cloud background containing 20 g/m$^2$ LWP. Both panels include calculations for low (solid black) and high (dashed) water vapor cases. Figure taken directly from [Daniel, et al., 2005].*

Intensity measurements were made using a photodiode array at 500 nm. This wavelength is chosen as a window where water absorbtion is low and the light received by the detector is a function of the atmospheric scattering primarily. In the microwave wavelength region emission is measured, the signal is dependent upon the amount of water in the column, and is essentially independent of size of the particles. Figure 3 depicts how a 'cloud' interacts spectrally with the different wavelengths.

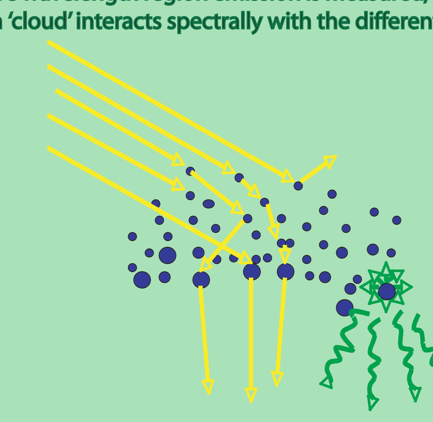

*Figure 3: Schematic displaying incoming solar radiation (yellow rays) being scattered and absorbed (these are the processes that the near infrared spectra and the intensity measure). The microwave emission of the water molecules, independent of droplet size and number, is depicted by the green rays.*

The LWP was determined by the microwave measurements then combined with the NIR measurements of PLWP to retrieve the effective radius. Three minute averages were made for each of the measurements to avoid differences that arise from the different spatial sampling of the two instruments. No retrieval was performed when the PLWP was under 100 $gm^{-2}$. Figure 6 displays the combined microwave and NIR radii retrieval results. The retrieved radii are higher than would be expected, and it is expected that a positive bias of 50 $gm^{-2}$ that was applied to align the PLWP with the LWP was insufficient to account for the bias that exists between the LWP, PLWP and the model values.

Figure 7 displays the radii and LWP retrieved from the combination of the intensity and PLWP measurements. 3 minute results are also presented to be comparable with figure 6 even though the intensity and the spectral measurements have the same field of view (see right photograph in figure 5) and higher temporal resolution is possible. Unlike the microwave-NIR combination where the path enhancement (PLWP/LWP) is the measurement, the intensity-NIR retrieval treats both the intensity and PLWP as measurements and the radius and LWP are simultaneously retrieved. The radii retrieved using the intensity-NIR method have almost a gaussian distribution with a peak about 12 µm, and similarly the LWP distribution is different from the microwave derived distribution. A calibration correction was required to be applied to the intensity measurements to allow consistency with model calculations. Calibration was performed using a lamp which was then externally calibrated to an absolute value ($Wm^{-2}nm^{-1}$).

## Conclusions and Outlook

A new method for deriving effective radius is presented and applied to measurements made at Barrow, Alaska in September, 2004
Combining intensity and PLWP measurments allows a microwave independent retrieval of LWP
Biases between the microwave, NIR and absolute calibration intensity measurments have the potential to be derived and provide validation
Aerosol indirect effect studies will require additional information on the aerosol to be added to this work's retrieval of LWP and radii

## References

Daniel, J.S., R. W. Portmann, H. L. Miller, A. L. Langford, C. E. Eubank, R. Schofield, D. D. Turner and M. D. Shupe, Cloud property estimates from zenith spectral measurements of scattered sunlight between 0.9 and 1.7 µm, Journal of Geophysical Research, Submitted 2005.
Kim, B. G., et al. (2003), Effective radius of cloud droplets by ground-based remote sensing: Relationship to aerosol, Journal of Geophysical Research-Atmospheres, 108.
Marchand, R., et al. (2003), An assessment of microwave absorption models and retrievals of cloud liquid water using clear-sky data, Journal of Geophysical Research-Atmospheres, 108.
Min, Q. L., and M. Duan (2005), Simultaneously retrieving cloud optical depth and effective radius for optically thin clouds, Journal of Geophysical Research, 110, DOI:10.1029/2005JF006136.
Min, Q. L., and L. C. Harrison (1996), Cloud properties derived from surface MFRSR measurements and comparison with GOES results at the ARM SGP site, Geophysical Research Letters, 23, 1641-1644.
Oreopoulos, L., et al. (2000), A new normalized difference cloud retrieval technique applied to landsat radiances over the Oklahoma ARM site, Journal of Applied Meteorology, 39, 2305-2321.
Rodgers, C. D. (2000), Inverse methods for atmospheric sounding, theory and practice, 1 ed., 0-238 pp., World Scientific Publishing Co. Pte. Ltd., Singapore.
Rosenfeld, D. (2000), Suppression of rain and snow by urban and industrial air pollution, Science, 287, 1793-1796.
Stamnes, K., et al. (1988), Numerically Stable Algorithm for Discrete-Ordinate-Method Radiative-Transfer in Multiple-Scattering and Emitting Layered Media, Applied Optics, 27, 2502-2509.
Twomey, S. (1974), Pollution and Planetary Albedo, Atmospheric Environment, 8, 1251-1256.
Wiscombe, W. J. (1980), Improved Mie Scattering Algorithms, Applied Optics, 19, 1505-1509.

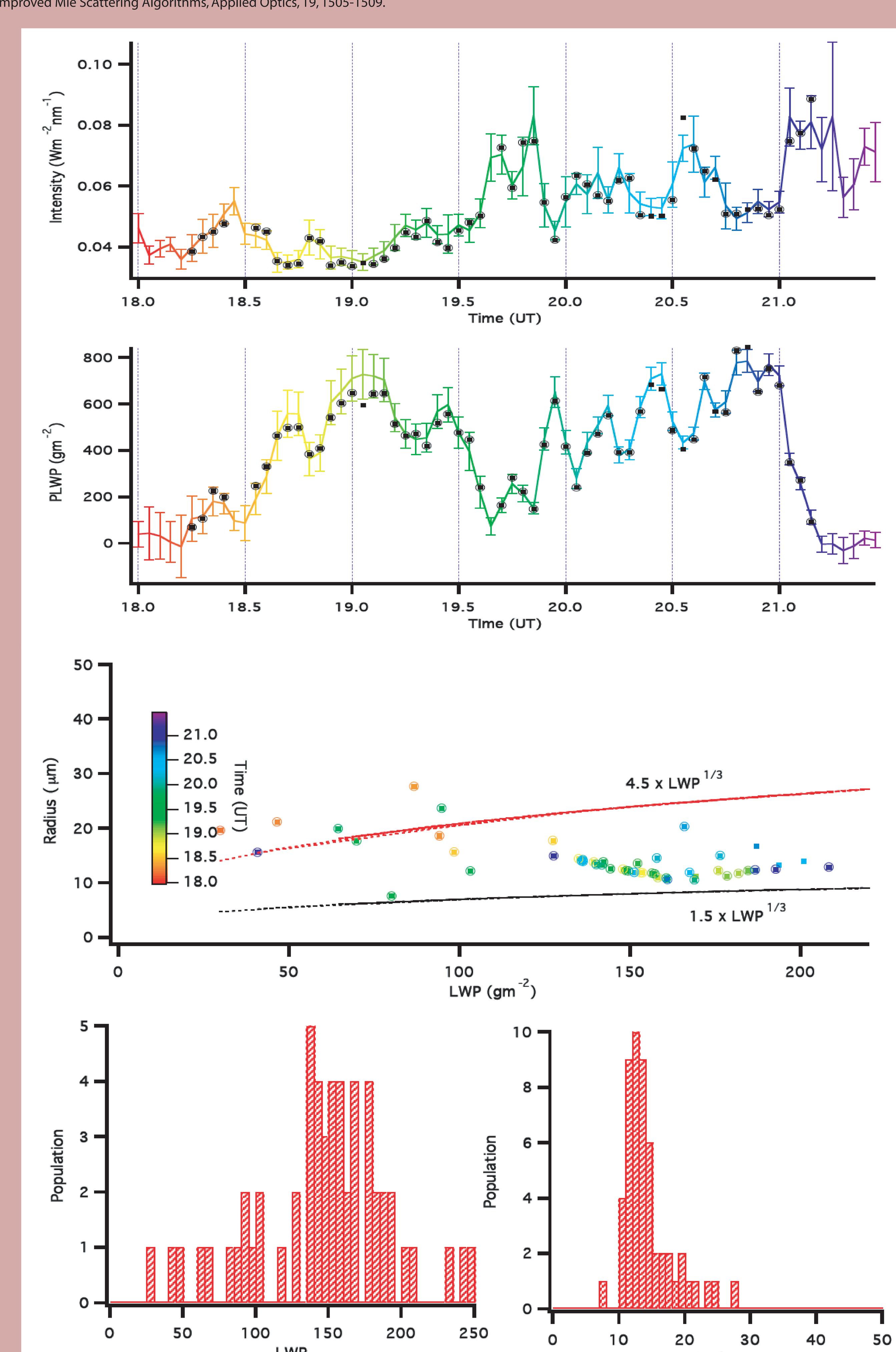


*Figure 7: Combined intensity and PLWP retrieval results. Upper panel depicts the intensity for 14th September, 2004 from 18-21.5 UT. 2nd panel depicts the PLWP and model fit (black dots (with circles indicating convergence)). The 3rd panel displays the retrieved radii and the lower panels give the distribution of the LWP and radii.*